Contribution from a eutrophic temperate estuary to the landscape flux of nitrous oxide

Emeline Lequy, Eero Asmala, Andreas Ibrom, Benjamin Loubet, Raia Silvia Massad, Stiig Markager, Josette Garnier

Water Research 222 (2022) 118874

Contents lists available at ScienceDirect

Water Research

journal homepage: www.elsevier.com/locate/watres

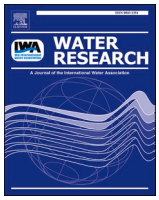

Contribution from a eutrophic temperate estuary to the landscape flux of nitrous oxide

Emeline Lequy [a,b,1,*], Eero Asmala [c], Andreas Ibrom [b], Benjamin Loubet [a], Raia Silvia Massad [a], Stiig Markager [d,2], Josette Garnier [e,2]

[a] Université Paris-Saclay, INRAE, AgroParisTech, UMR ECOSYS, Thiverval-Grignon 78850, France
[b] Technical University of Denmark (DTU), Environmental Engineering, Roskilde, Denmark
[c] Geological Survey of Finland, Espoo, Finland
[d] Aarhus University, Roskilde, Denmark
[e] Sorbonne Université-CNRS-EPHE, UMR METIS, BP 105, Tour 56-55, Etage 4, 4 Place Jussieu, Paris 75005, France

ARTICLE INFO

Keywords:
Greenhouse gas
Water-atmosphere interface
Statistical modeling
Eddy covariance
Roskilde Fjord

ABSTRACT

For mitigation of climate change, all sources and sinks of greenhouse gases from the environment must be quantified and their driving factors identified. Nitrous oxide (N_2O) is a strong greenhouse gas, and the contribution of aquatic systems to the global N_2O budget remains poorly constrained. In this study, we measured N_2O concentrations in a eutrophic coastal system, Roskilde Fjord (Denmark), and combined measurements with statistical modeling to quantify the N_2O fluxes and budget in the system over a period of six months. To do so, we collected water at 15 sampling points and measured N_2O concentrations along with physico-chemical water quality parameters, *e.g.* temperature, salinity, dissolved inorganic nitrogen and phosphorus, and silicon. We used mixed-effect regression models to predict N_2O concentrations in the water from water quality parameters. We then derived N_2O fluxes using well-established equations of N_2O solubility and water-atmosphere exchanges. These fluxes were then put in perspective with those measured at the landscape scale by eddy-covariance at a 96 m nearby tall tower, and to those estimated from the agricultural land next to the fjord using Intergovernmental Panel on Climate Change (IPCC) guidelines. N_2O concentrations in the Roskilde Fjord ranged between 2.40 and 8.05 nmol l^{-1}. The best fitting model between water parameters and N_2O concentrations in water included phosphorus and temperature. We estimated that (i) Roskilde Fjord was a sink of N_2O, with a median inward flux of -0.04 nmol m^{-2} s^{-1}, (ii) while the surrounding median agricultural flux was 0.13-0.18 nmol m^{-2} s^{-1}, and (iii) the median landscape flux was 0.07 nmol m^{-2} s^{-1}. All estimates of N_2O fluxes were of the same magnitude and consistent with each other. These preliminary results need to be consolidated by further research.

1. Introduction

Nitrous oxide (N_2O) is a potent and long-lived greenhouse gas, and the third contributor to global anthropogenic radiative forcing (0.17 [0.14 to 0.20] W m^{-2}), which amounts 6.4% of the total anthropogenic forcing (Myhre et al., 2013). N_2O has a wide range of anthropogenic and natural sources (IPCC, 2013). Assessing the contribution of water systems, especially eutrophicated ones, to the global budget of N_2O emissions is necessary for monitoring and understanding sources, sinks and drivers of N_2O atmospheric concentrations, and to decide on mitigation strategies. Among semi-natural systems, oceans and coastal systems are considered important sources of N_2O, with *ca.* 10% of total emissions (Turner et al., 2015); yet the observations vary considerably between studies, which investigated contrasted ecosystems (from temperate estuaries to mangroves), and included a limited spatial and temporal coverage (Bange, 2006; Garnier et al., 2009; Murray et al., 2015).

N_2O production in aquatic environments results from microbiological activity that highly depends on the oxygen conditions and the availability of nitrogen – as ammonium, nitrite, nitrate and nitrogen bound in organic matter (Murray et al., 2015). Estuaries and coastal

* Corresponding author at: Université Paris-Saclay, INRAE, AgroParisTech, UMR ECOSYS, 78850, Thiverval-Grignon, France.
E-mail address: e.lequy@gmail.com (E. Lequy).
[1] Preent address: INSERM/UVSQ/U Paris Cité/U Paris-Saclay, UMS 011, 16 Avenue Paul Vaillant Couturier, F-94807 Villejuif, France.
[2] These authors contributed equally to this study.

https://doi.org/10.1016/j.watres.2022.118874
Received 20 December 2021; Received in revised form 22 June 2022; Accepted 14 July 2022
Available online 16 July 2022

systems receive large amounts of anthropogenic inputs of nitrogen (Cloern, 2001) – especially in landscapes with high agricultural activities (de Vries et al., 2011). This nitrogen increases primary production, favoring accumulation of organic matter in the water column and at the sea floor (Markager et al., 2011), which is degraded into inorganic nitrogen through mineralization and further processes including nitrification and denitrification possibly producing N_2O. Indeed N_2O production has been shown to increase in sub-optimal conditions of oxygen tension both in the case of nitrification (Bie et al., 2002; Cébron et al., 2005) and denitrification (Tallec et al., 2006). Therefore apparently "autochtonous" nitrogen may originally come from external inputs (Asmala et al., 2018; Knudsen-Leerbeck et al., 2017). For this reason, N_2O emissions from water systems are considered "indirect emissions" derived from human activities, along with losses from agricultural fertilization, considered as direct ones. These indirect emissions may substantially contribute to total emissions at various scales, from river basins (Borges et al., 2018; Marescaux et al., 2018) to the global scale (Smith, 2017).

However, N_2O fluxes in aquatic ecosystems remain poorly quantified (Bange et al., 2009), because of technical constrains associated with the highly variable fluxes of N_2O in space and time. Indirect emissions may cause large uncertainties in N_2O budgets (Smith, 2017). Therefore, more measurements from different approaches are needed to improve the spatial and temporal coverage of data for N_2O fluxes from aquatic systems (IPCC, 2006, and following IPCC reports). Estimating N_2O fluxes from or to aquatic ecosystems relies on several techniques: direct measurements by floating chambers, small to landscape scale measurements by eddy covariance, or calculations derived from N_2O concentrations measured in the water. All methods present shortcomings: floating chambers and N_2O concentration measurements at specific sampling points cannot cover large areas or yield high frequency time-series, while fluxes based on eddy covariance measurements rely on several uncertain assumptions on source locations. Combining independent methods at different spatial scales and temporal resolution offers an option to collect the best possible estimates of estuarine N_2O fluxes, as previously done with other greenhouse gases (Eugster et al., 2003; Morin et al., 2017; Podgrajsek et al., 2014; Schubert et al., 2012).

In this study, we measured N_2O water concentrations in the Roskilde Fjord and aimed at (i) statistically modeling N_2O water concentrations over the study period, and (ii) inferring the corresponding time-series of N_2O fluxes. As secondary objective, to internally evaluate the credibility of the estimated N_2O fluxes of Roskilde Fjord, we put these fluxes in perspective with eddy covariance measurements carried out for the same study site, including a nearby agricultural area, for which we also estimated N_2O fluxes. This study is among the first attempts to use eddy covariance at the land-sea interface to assess N_2O emissions in a heterogeneous coastal landscape.

2. Material and methods

2.1. The sampling site and sampling design

Roskilde Fjord is a temperate eutrophic estuary (Pedersen et al., 2014) and a branch of the Isefjord in the Zealand Island, Denmark (55°41.5N; 12°04.92E). Roskilde Fjord is a long, narrow (width≈0.5-10 km, length≈40 km), and shallow (≈3 m) estuary flowing into the Kattegat (Fig. 1). This estuary divides into two parts and the present study was conducted in the southern inner part of the Roskilde Fjord, where salinity is moderate (≈ 14 g kg^{-1}) and the residence time up to one year (Flindt et al., 1997). There are no large rivers flowing into the Roskilde Fjord: the freshwater comes from five small creeks (1116 l s^{-1}), submarine groundwater discharge (flow unknown), and from a wastewater treatment plant serving the city of Roskilde (237 l s^{-1}) (Pedersen et al., 2014).

A 125-m-tall tower at the Risø Campus of the Technical University of Denmark (55.69°N, 12.09°E) on the eastern shore of Roskilde Fjord was equipped in July 2014 with an eddy covariance sensor at 96 m high to monitor N_2O fluxes from the surrounding landscape. Flux footprint estimations based on micrometeorological measurements and the footprint model by Kormann and Meixner (2001) indicated a range between 0 and 5 km (daytime) and >10 km (night) around the tower. For this reason, the present study was limited to these first 5 km. The winds predominantly come from south-west and westerly directions and the footprint area includes 36 km^2 of the inner Roskilde Fjord (46% of the daytime footprint).

To achieve our objectives, we used two datasets in parallel: one to build statistical models to explain concentrations of dissolved N_2O in water, and one to predict N_2O dissolved concentration in water from these statistical models, and to calculate subsequent N_2O fluxes over the 6-month study period. To build statistical models, we used data measured at a set of sampling sites chosen to cover the study area: 15 sampling points distributed on a rough grid (Fig. 1). Three sampling surveys were conducted on the 1st of May, 8th of July, and 17th of September 2014 at each of these sampling sites. To predict time-series of N_2O concentrations and N_2O fluxes, we used the data collected at a long-term water monitoring station corresponding to sampling site 2.

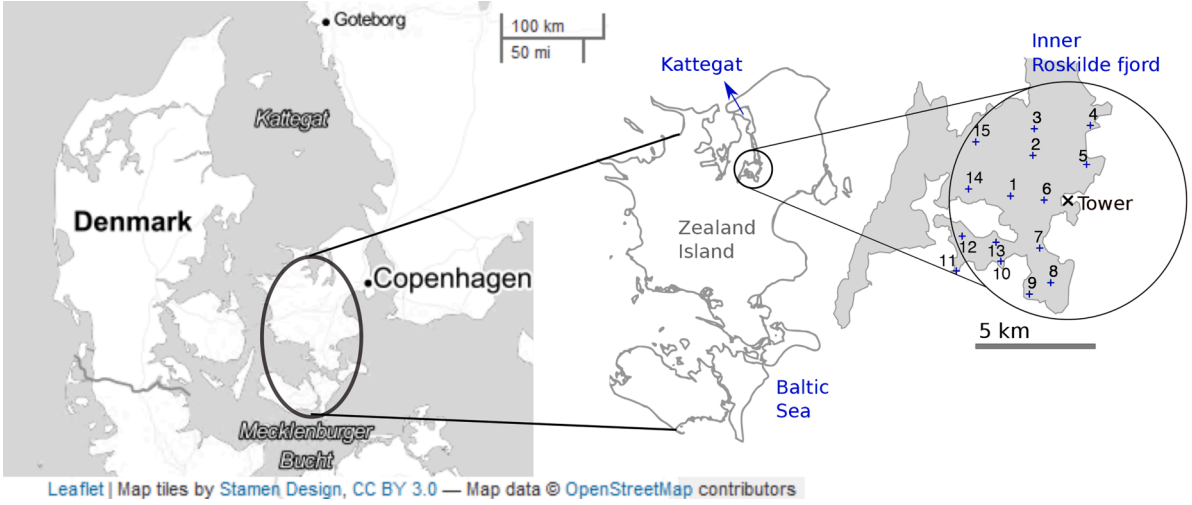

Fig. 1. Sampling area within the 5-km radius circle (circle on the right panel) around the tall tower at the Risø campus (depicted as the cross on the right panel, equipped with eddy covariance sensor at 96m high) on the Danish Zealand Island, and spatial distribution of the 15 sampling points over the inner Roskilde Fjord (blue dots), which flows to the Kattegat (the blue arrow in the center panel).

2.2. Chemical analyses

2.2.1. Water samples at the 15 sampling points in May, July, and September

Water sampling was carried out by collecting 2 l of water at 1m depth using a standard Ruttner water sampler (11.003 series, 3 L). We simultaneously measured temperature and salinity, also at 1 m depth, with a handheld field multiprobe (YSI ProDSS, YSI, Yellow Springs, OH, USA).

A set of water samples were analyzed for dissolved NO_2^-, NO_3^- and NH_4^+, dissolved silicon (DSi), and dissolved inorganic phosphorus (DIP). Triplicate samples were taken at each sampling points in 30 ml acid washed plastic bottles and brought to the laboratory within two hours where they immediately were frozen to prevent any nitrogen consumption. These samples were analyzed by Scalar Continuous Flow Analyser (San ++) as described by Cauwet (1999) and Holmes and colleagues (1999). Detection limits were 0.04, 0.1, 0.3, 0.06 and 0.2 μmol l^{-1} for NO_2^-, NO_3^-, NH_4^+, DIP and DSi, respectively.

In this study, N_2O concentrations were analyzed for the first time in Roskilde Fjord. To constitute this first dataset of N_2O concentrations in water, another set of water samples was collected: at each sampling point, a clean 150-ml glass bottle was rinsed then gently filled with sampled water, avoiding any bubble. We added a few droplets of a 5 % solution of $HgCl_2$ to stop all living activity and sealed the bottles. The samples were shipped right after sampling to the UMR METIS (CNRS, France) where they were stored refrigerated until analysis, as follows. A water sample aliquot (20 ml) is used for determination of N_2O in triplicates with a gas chromatograph (GC Perichrom ST 200) equipped with an electron capture detector. The detection limit is of ~1 nmol N_2O l^{-1} (Garnier et al., 2009). The water sample is introduced in a degassing chamber through which a gaseous mixture of argon - methane 90/10 passes and carries away the dissolved N_2O. This carrier stream contains water vapor which is eliminated in a glass tube filled with silica-gel inserted upstream the N_2O concentrator trap required before the connection to GC. Therefore, the sweep gas passes through a molecular sieve trap cooled to -120°C by liquid nitrogen. A switch valve puts then in communication the trap concentrator and the chromatographic column. An ultra-fast heating of the trap allows to reach 200°C, temperature at which the desorption of N_2O is complete and almost instantaneous. Calculations are based on calibrations done at least four times with a standard gas.

2.2.2. Water measurements at the long-term monitoring site

At a 34-year old long-term water quality monitoring site corresponding to sampling point 2 of the present study, the following concentrations were measured biweekly: dissolved NO_2^-, NO_3^- and NH_4^+ for nitrogen; DSi and DIP; temperature and salinity; and chlorophyll a (Conley et al., 2002; Riemann et al., 2016). Here we only used the 6-month period corresponding to our N_2O sampling campaigns.

2.2.3. Atmospheric N_2O flux measurements

The eddy covariance system consisted of an Off-Axis Integrated-Cavity Output Spectroscopy laser analyzer (Model N2O/CO-23d, Los Gatos Research, Mountain View, USA) and a 3D ultrasonic anemometer (USA-1, METEK, Elmshorn, Germany). The analyzer measured N_2O, CO and H_2O dry mixing ratios: this enabled correcting for water vapor dilution effects (Ibrom et al., 2007). Air was sampled at 96 m via a 150 m long Nylon tube with an inner diameter of 8 mm at a rate of 29.6 l min^{-1} using a vacuum pump (XDS-35i, Edwards, Crawley, UK). The turbulence data were sampled at 10 Hz. The fluxes were processed with the RCPM software including post-processing routines (Morgenstern, 2000). Measurements started in July 2014, with gaps caused by pump and computer breakdowns. For this study, we selected five months of valid tower data between July and November 2014 (missing data = 8%). Wind speed was measured at 44.2, 76.6, 94, 118, and 125 meters height. The wind speed followed a natural logarithmic profile and we extrapolated it to 10 meters high for calculating the water-air exchange coefficients. Due to uncertainties in the estimation of the footprint, we chose to only use daytime data in sectors that cover the Roskilde Fjord (western wind direction, *i.e.* 0-35° and 195-360°).

2.3. Statistical analyses and modeling of N_2O concentrations in water

Beyond the descriptive analysis, our statistical analyses aimed to (i) build models to explain the N_2O concentrations in the Roskilde Fjord water from other water quality variables, and (ii) use these models to predict N_2O concentrations in our study site. From these predicted concentrations, we aimed to estimate N_2O fluxes from Roskilde Fjord based on equations relying on temperature, salinity, wind speed and other variables onsite, and to compare these values and their corresponding seasonal budget (i) to the eddy covariance measurements over the 5-km radius fetch of the tall tower and (ii) to a budget for the agricultural landscape calculated following the IPCC calculations guidelines.

We performed Kruskal-Wallis tests to compare the water characteristics between the three surveys. We aimed at building two statistical models to predict N_2O concentrations: the most simple one (thereafter referred to as "simplistic"), and the best goodness-of-fit one. The simplistic one was designed to estimate N_2O water concentration as simply as possible using only temperature as detailed below. The goodness-of-fit one was designed to gain insight in the possible mechanisms involved in N_2O production while being capable of predicting N_2O concentrations in the Roskilde Fjord, from the variables available in the study area, and with the best predictive power. The predicted N_2O concentrations by each model, as well as the N_2O fluxes derived from them, were compared to evaluate whether the simplistic model could be a valid option for monitoring sites with little equipment.

Since we used repeated measurements (May, July, and September) in 15 sampling points over Roskilde Fjord, thus violating the assumption of independency, we used a mixed model able to account for such hierarchical structure, including a random intercept for the sampling site and fixed effects for all the other variables (Wood, 2006; Zuur et al., 2009a, 2009b). To test for any non-linear relationships, we also chose generalized additive mixed modeling with spline functions for all continuous variables, therefore accounting for any non-linear relationship. To ensure a normal distribution of the residuals and homoscedasticity in the models, as well as non-negative concentrations of predicted N_2O, we log-transformed N_2O concentrations in the modeling analyses (we back-transformed the outputs of the model in the subsequent analyses).

We assumed that, since temperature strongly controls microbial activities, it would have the strongest effect on N_2O dynamics of all available variables. So, in the first approach ('simplistic'), we built the simplest model by using log-transformed N_2O as response variable with only temperature as explanatory variable. In the second approach ('best quality-of-fit'), we performed a stepwise variable selection to obtain the best goodness of fit and most parsimonious model adjusted for other variables. For this reason, we started our variable selection by adjusting for NO_2^-, NO_3^-, NH_4^+, or DIN in separate models, and then we further adjusted for DSi and DIP to better take into account the role of eutrophication. Finally, as the simplistic approach revealed a large effect of temperature, we adjusted for temperature. We selected the best quality-of-fit model according to (i) the Akaike information criterion (AIC) – the lower, the better the quality of fit, and (ii) results of ANOVA between models by increasing complexity.

Statistical analyses were performed using R version 3.3.2 (R Core Team, 2015) and the package 'MGCV' (Wood, 2006).

2.4. Time-interpolation of the data

We aimed to construct a time-series of the N_2O fluxes between the aquatic system of Roskilde Fjord, at the long-term monitoring station of water quality corresponding to sampling point 2, and the atmosphere. First, to reconstruct N_2O concentrations by statistical modeling over our

6-month study period, we used the values of water parameters obtained close to monitoring station 2. Since measurements of temperature, salinity, DSi and DIP were conducted on a bi-weekly frequency, we linearly interpolated with a half hourly time-step to match the frequency of the tall tower measurements used in the N_2O flux calculations described hereafter.

Given that the three surveys were conducted between May and September 2014, we defined a validity period for the predicting models based on the water temperature of the Roskilde Fjord. We estimated that the models were reliable for temperatures ±3°C above and below the maximum and minimum measured water temperatures, between 10 and 25°C. The resulting study period was six months, between April the 16th and October the 31st of 2014.

2.5. Nitrous oxide flux calculations at sampling point 2

We calculated the N_2O fluxes from Roskilde Fjord to atmosphere using the following equation:

$$F_{N_2O} = k_w(u).(C_w - C_e), \quad (1)$$

where $k_w(u)$ is the gas transfer velocity (m s^{-1}) as a function of wind speed (u in 10m height), C_w is the concentration measured or modeled in the water and C_e is the equilibrium concentration of N_2O (calculation described hereafter).

The gas transfer velocity, k_w, was calculated based on equations depending on three classes of wind speed as detailed in the synthesis by Bange et al. (2001). We used the equations of Weiss and Price (1980) to compute C_e as following:

$$C_e = x_{N2O}.B.P, \quad (2)$$

where x_{N2O} is the dry molar fraction of N_2O in the atmosphere measured by the eddy covariance sensor, B is the Bunsen solubility (calculated from temperature and salinity) and P is the atmospheric pressure (also from the eddy covariance sensor). All the equations allowing for estimation of the variables needed for calculating N_2O fluxes necessarily caused some uncertainty and error propagation (Bange et al., 2001).

2.6. Towards generalization of the results over the 15 sampling points

Because the long-term data collected in the monitoring station at sampling point 2 was not available at the other 14 sampling sites, we compared sampling point 2 to the other 14 sampling points in term of water temperature and concentrations in water. In an attempt to generalize our findings at sampling point 2, we conducted sensitivity analyses to predict N_2O concentrations under the range of temperature, salinity, and water parameters collected in the 15 sampling sites, and to calculate the corresponding N_2O fluxes. To do so, we applied the exact same methodology as those described above, but used several datasets in which we added or removed 10% to salinity, temperature, and DIP, in several combinations.

2.7. Nitrous oxide flux from the agricultural areas

We gathered information for all registered crops for 2014 in our study area (surface, type of crop, authorized maximal fertilization rate). We used the following simplified IPCC-Tier 1 equation to compute the direct emissions from agriculture (Hergoualc'h et al., 2019):

$$\mathrm{FN2O} = \sum_i EFi.\mathrm{FNi} \quad (3)$$

where i is the index of crops or pastures, EF is the emission factor, and FN is the amount of fertilizer; EFi took the values of 0.81% and 1% of the nitrogen applied in each crop and grassland, respectively (Chirinda et al., 2010), and we considered all nitrogen inputs to be synthetic fertilizers.

To complete this simplified calculation, we used the formula developed by Garnier et al. (2019) that estimates, at landscape scale, N_2O emissions from agricultural areas. This formula is based on temperature and rainfall, and input fertilizers (Supplementary Materials). For our study site and period, we used 11°C as average annual temperature, and 650 mm yr^{-1} as annual rainfall.

As a supplementary analysis, to distinguish daytime measurements of N_2O at the tall tower coming either from Roskilde Fjord or from the agricultural area, we proceeded as follows. To estimate agricultural fluxes, we selected measurements of N_2O fluxes at the tall tower coming only from the Northeast of the tower, defined as 30-100°. To estimate fluxes coming from Roskilde Fjord, we selected measurements of N_2O fluxes at the tall tower coming only from between 270 and 360°, the area including the less agricultural areas.

3. Results

3.1. Water characteristics in the Roskilde Fjord

3.1.1. Characteristics during the three surveys at the 15 sampling points

The three surveys showed significantly different concentrations of NO_3^-, NO_2^-, NH_4^+, DIP and DSi (Table 1). In May, after the spring bloom (usually in March), both DIP and dissolved inorganic nitrogen (DIN) concentrations were low and often with a pronounced P-limitation. In July, DIP concentrations increased (due to release from the anoxic sediments), whereas DIN concentrations were still low. DIN concentrations increased in September (when phytoplankton production started to be light-limited). DSi was never limiting for production. Temperature followed irradiance and air temperature with a maximum in July-August. Salinity only displayed small fluctuation (driven by wind-forced exchanges with the Kattegat). In particular, temperature, salinity, and DIP at sampling point 2 fell in the range of those measured at the other 14 sampling points, albeit with a difference of around 10-20% with the median (Supplementary Fig. S1)

3.1.2. Interpolated time-series at the sampling point 2

The interpolated temperature, DIP, and DSi followed large seasonal variations (Fig. 2). As suggested by our three samplings, temperature globally followed a hill-shaped curve from May to October at the

Table 1
Concentrations of dissolved inorganic nitrogen (DIN: NO_3^-, NH_4^+ and NO_2^-, dissolved inorganic phosphorus (DIP) and dissolved silicon (DSi), and measured temperature and salinity in the Roskilde Fjord during the three sampling campaigns (median and interquartile range between brackets). The p-values are from Kruskal-Wallis tests.

Variable	unit	May N=15	July N=15	September N=15	p
NO_3^-	µmol l^{-1}	0.26 [0.18, 0.55]	0.01 [0.00, 0.07]	1.20 [0.82, 1.53]	<0.001
NO_2^-	µmol l^{-1}	0.04 [0.03, 0.05]	0.01 [0.01, 0.04]	0.27 [0.25, 0.28]	<0.001
NH_4^+	µmol l^{-1}	1.43 [1.10, 1.77]	0.18 [0.14, 0.29]	2.87 [1.30, 3.49]	<0.001
DIP	µmol l^{-1}	0.92 [0.82, 1.04]	7.70 [7.45, 8.09]	7.80 [7.78, 8.01]	<0.001
DSi	µmol l^{-1}	35.73 [32.24, 46.75]	39.12 [36.52, 41.99]	150.62 [144.70, 158.67]	<0.001
Salinity	g kg^{-1}	14.49 [13.95, 14.64]	15.02 [14.34, 15.16]	15.28 [14.81, 15.42]	0.002
Temperature	°C	14.70 [14.60, 14.75]	21.50 [21.25, 21.75]	16.80 [16.70, 17.15]	<0.001
DSi:DIP	-	47.24 [34.88, 54.29]	5.24 [4.68, 5.51]	19.12 [17.72, 19.86]	<0.001

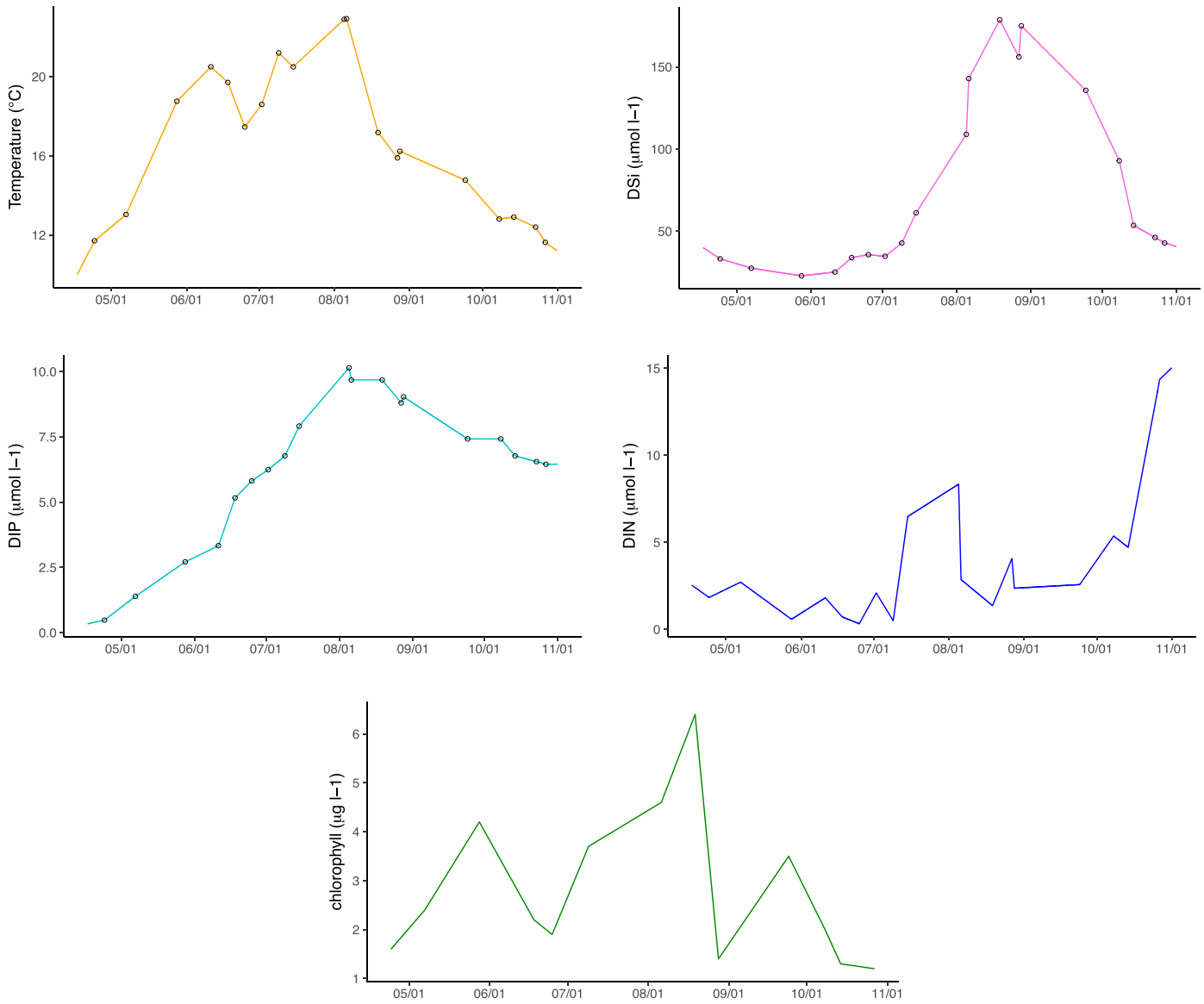

Fig. 2. Time-series of linearly interpolated temperature, dissolved silicon (DSi), dissolved inorganic phosphorus (DIP), dissolved inorganic nitrogen (DIN), and of chlorophyll a in the Roskilde Fjord between April and October 2014 at the monitoring station corresponding to sampling point 2.

sampling point 2, with a sudden decrease in July. DIP gradually increased from 0 to almost 10 µmol l^{-1} from May to the end of July then gradually decreased to 7 µmol l^{-1}. DSi stagnated below 50 µmol l^{-1} until early July, where it increased quickly above 150 µmol l^{-1} in August and decreased also quickly from September to November, again below 50 µmol l^{-1}. For comparison, indicative half saturating constant for phytoplankton growth are 0.2, 1 and 2 µmol l^{-1} for DIP, DIN and DSi, respectively (Hinsby et al., 2012).

We used these interpolated temperature and phosphorus variables to estimate N_2O concentrations using the simplistic and the best-quality-of-fit models as described hereafter.

3.2. N_2O concentrations

3.2.1. Concentrations at 15 sampling sites over the Roskilde Fjord

The median N_2O concentrations were 3.65 [interquartile range (IQR): 3.49, 3.93], 2.81 [2.70, 2.91], and 5.87 [5.72, 6.06] nmol l^{-1} in the May, July, and September surveys, respectively (Fig. 3). We observed a maximal value of 8.0 nmol l^{-1} at the sampling point 1 on May 1st. We considered it as an outlier because it was larger than the median plus 10 times the interquartile range, and we discarded it from the rest of the statistical analyses. After removing this outlier, nitrous oxide concentration ranged between 2.4 and 6.4 nmol l^{-1} in the Roskilde Fjord between May and September 2014, with a median of 3.6 nmol l^{-1} (IQR: 2.8 nmol l^{-1}). A Kruskal-Wallis test indicated that the three surveys differed significantly ($p<0.001$). N_2O correlated well with NO_2^-, NO_3^- and NH_4^+ with significant Spearman rho coefficients of 0.70, 0.68, and 0.69 ($p<0.001$), respectively.

3.2.2. Predicting time-series of N_2O concentrations at sampling point 2

Simplistic approach: in this approach aiming at using only temperature, the model indicated a significant non-linear effect of temperature. The smooth term showed around six estimated degrees of freedom (Table 2), indicating six changes of the curve inflection throughout our range of measured temperatures (Fig. 4). As the linear assumption was violated for temperature, we chose to keep the spline function in the final simplistic model. The R^2 of this model was 0.92 (AIC: -56).

Best quality-of-fit approach: in this approach, we included at first

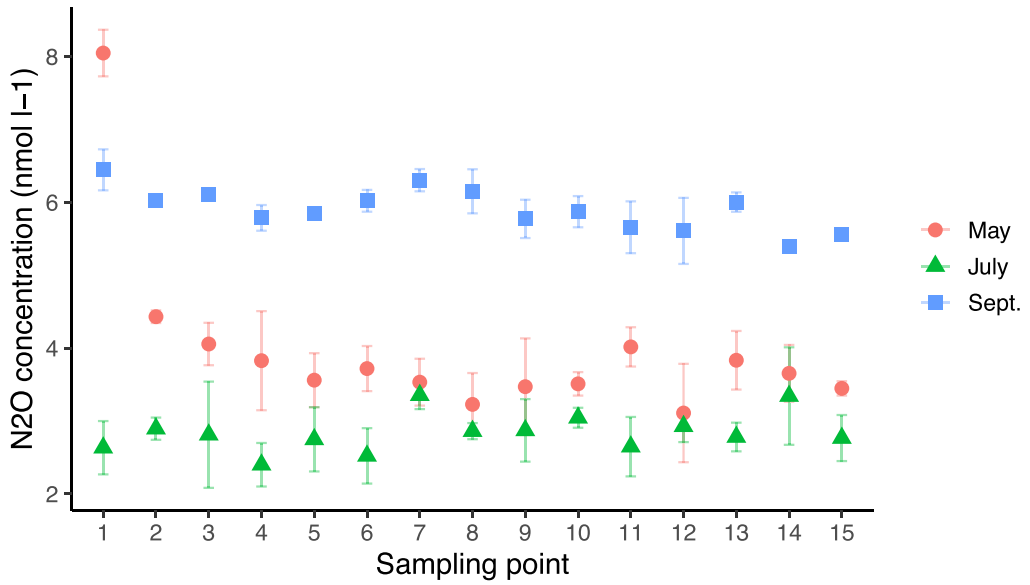

Fig. 3. Concentrations of N_2O (nmol l^{-1}, mean ± standard deviation) at the 15 sampling points over the Roskilde Fjord measured in May, July, and September 2014. Triplicate measurements at sampling point 1 in May were considered outliers.

Table 2
Results of the spline variable "temperature", and coefficient estimate of dissolved phosphorus (P), computed by the simplistic and the best quality-of-fit models. Edf stands for estimated degrees of freedom and represents the number of inflexions of the curve between natural log-transformed N_2O concentrations and temperature (see Fig. 4). N=15 sampling sites.

Model	Non-linear relationships			Linear relationships			
	Variable	edf	p-value	Variable	Estimate	Standard error	p-value
Simplistic	temperature (°C)	6.55	<0.001	-	-	-	-
Best quality-of-fit	temperature (°C)	5.55	<0.001	DIP (μmol l^{-1})	0.074	0.017	<0.001

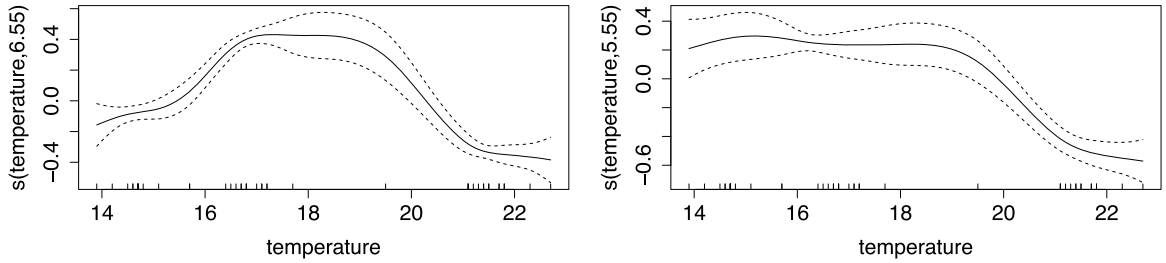

Fig. 4. Representation of the non-linear effect of the water temperature (X axis, in °C) on the log-transformed concentrations of N_2O in our samples (Y axis, partial residuals of centered natural-log transformed N_2O concentrations) from the models described in Table 2. The solid and dotted lines represent the average effect of temperature on the concentrations of N_2O and its standard deviation, respectively. Left: simplistic model; right: best quality-of-fit model.

nitrogen variables in separate models, but each of NO_3^-, NH_4^+ and NO_2^- were largely confounded by DIP, and even more by temperature, as these models yielded small and non-significant regression coefficients for nitrogen variables. Pooling the three nitrogen variables into one DIN variable yielded similar results. Therefore, the final best-quality-of-fit model included only temperature and DIP, both included with a spline function to account for possible non-linearity. The R^2 of this model was 0.94 (AIC: -70). Adding DSi did not significantly improved the model (R^2: 0.93, AIC: -71). We found a significant non-linear effect for temperature, and the model indicated five changes of the curve inflection (Table 2 and Fig. 4). We removed the spline function for DIP because this model did not show any statistically significant deviation from linearity, therefore obtaining a significant and positive coefficient for DIP. Table S1 provides examples of predicted N_2O water concentrations using the "best quality-of-fit" model for selected values of temperature and DIP.

The predicted N_2O concentrations showed slightly different temporal patterns between the two models (Fig. 5), with a similar order of magnitude and a significant correlation between the two time-series (Spearman rho coefficient of 0.55, $p<0.001$).

Despite excellent agreement between the measured and modelled N_2O concentrations (Fig. S2), at sampling point 2 for the May survey we found a measured N_2O concentration somewhat higher than the predicted ones with the best quality-of-fit and simplistic models. The predicted values are more consistent for the two other following surveys at sampling point 2 – especially the 'best quality-of-fit' model.

3.3. *N_2O fluxes*

3.3.1. *Time-series over the Roskilde Fjord*

The two sets of estimated N_2O concentrations at the sampling point 2 of the Roskilde Fjord yielded very similar temporal patterns of N_2O fluxes (Fig. 6) with a significant Spearman correlation coefficient of 0.97

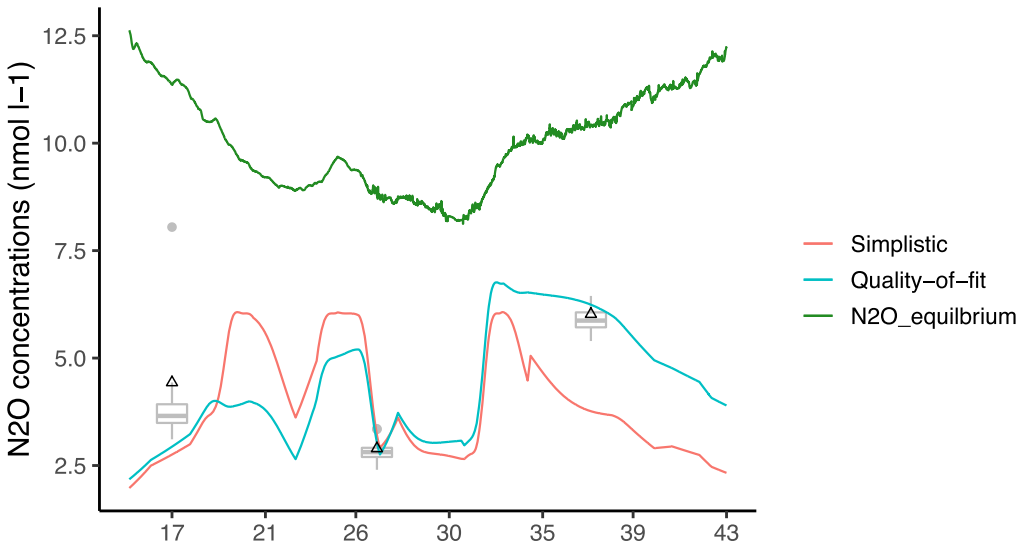

Fig. 5. Time-series of the modelled N_2O concentrations at sampling point 2 of Roskilde Fjord between April and October 2014 (from week 17 to 43) according to the simplistic and best-quality-of-fit models (including only temperature or temperature and DIP, respectively), and corresponding to C_w in Eq. (1), and time series of equilibrium N_2O concentration (C_e in Eq. (1)). The three triangles indicate N_2O concentrations at sampling point 2, and the three boxplots summarize the measured N_2O concentrations at all sampling sites combined for each survey. Boxes depict the 25th and 75th percentiles, the line in the box depicts the median, and all gray dots depict values out of the median±1.5 times the interquartile range.

($p<0.001$). Our results indicated that at this sampling point, the Roskilde Fjord only absorbed N_2O, with a median of – 0.04 [-0.08, -0.01] and -0.03 [-0.07, -0.01] nmol m^{-2} s^{-1} for the "simplistic" and the "best quality-of-fit" models, respectively, between April and December 2014 (and -0.05 [-0.09, -0.01] and -0.04 [-0.08, -0.01] nmol m^{-2} s^{-1} between July and December). The sensitivity analysis using temperature, salinity, and DIP increased or decreased by 10% in several combinations, to estimate N_2O concentrations at other locations in the inner Roskilde Fjord, did not change much the predicted N_2O fluxes with medians ranging from -0.06 to -0.04 nmol m^{-2} s^{-1} (Table S2).

The tall tower provided N_2O fluxes from July. In the period July-December, the daytime eddy covariance measurements on the tower, restricted to those coming from the West where the Roskilde Fjord lies, yielded a median flux of 0.07 [-0.04, 0.21] nmol m^{-2} s^{-1} (or 0.35 kg N ha^{-1} over this 6-month period).

3.3.2. *Agricultural N_2O fluxes*

The agricultural area was dominated by crops (77% of the agricultural surface), especially wheat and winter rapeseed. Fertilization ranged from 0 to more than 300 kgN ha^{-1} $year^{-1}$ (on average 126±76 kgN ha^{-1} $year^{-1}$). The simplified IPCC calculation and the landscape algorithm by Garnier et al. (2019) yielded N_2O fluxes of 0.13 and 0.18 nmol m^{-2} s^{-1}, respectively, from the agricultural area in the fetch of the tall tower (Fig. 6). This is also the same magnitude of the N_2O fluxes measured at the tall-tower, restricting measurements to daytime northeastern sector, of 0.06 [-0.01, 0.17] nmol m^{-2} s^{-1} (Fig. S3).

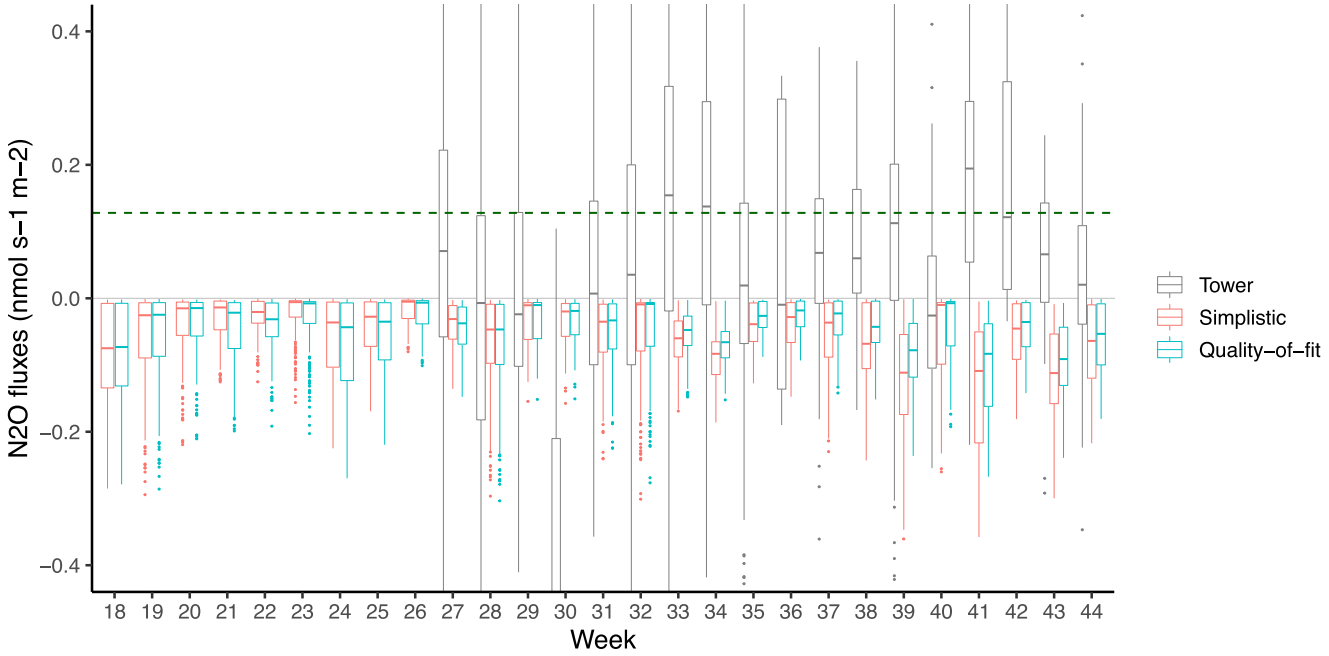

Fig. 6. Weekly distribution of the N_2O fluxes (nmol m^{-2} s^{-1}) estimated by the 'simplistic' model (in red, including only temperature) and by the 'best quality-of-fit' model (in blue, including temperature and DIP) at sampling point 2, and N_2O fluxes measured by eddy covariance at 96m high on the tall tower during daytime from western sectors (in grey, from week 27). The horizontal dotted line shows the average N_2O flux from the agricultural landscape of 0.13 nmol N_2O m^{-2} s^{-1} calculated using a simplified equation derived from the IPCC guidelines. Boxes depict the 25th and 75th percentiles, the line in the box depicts the median, and all the dots depict values out of the median±1.5 times the interquartile range.

4. Discussion

We estimated that the Roskilde Fjord could have absorbed N_2O at a median rate of -0.04 nmol m^{-2} s^{-1} at the sampling point between May and December 2014. This is compatible with the daytime eddy covariance data at 96 m high on the Risø tall tower (restricted to Western sectors), which measured N_2O fluxes in a daytime footprint of 5 km (median of 0.07 nmol m^{-2} s^{-1}), including a 24 km^2 large agricultural area, and with the estimated N_2O budget of this agricultural area (magnitude of 0.13-0.18 nmol m^{-2} s^{-1}).

4.1. The Roskilde Fjord overall status

The water characteristics measured in our study are in agreement with the past measurements of nutrients and salinity in the inner Roskilde Fjord between 2006 and 2013, with slightly higher average salinity (Staehr et al., 2017) and nutrient patterns typical of the Roskilde Fjord estuary (Knudsen-Leerbeck et al., 2017), and of shallow temperate estuaries in general.

Seasonally between 2006 and 2013, DIN and DIP varied from close to 0 to 70 μmol DIN l^{-1} and 10 μmol DIP l^{-1}, respectively. According to these past values, DIN and DIP concentrations were at their lowest during our three samplings (0.2 to 4.3 μmol DIN l^{-1}, and 0.9 to 7.8 μmol DIP l^{-1}, see Table 1), while higher concentrations could have been expected in winter time, before April and after October, i.e, at the time of nutrient replenishment and low biological uptake. The quality of water in the inner Roskilde Fjord has been improving since 1990, with nitrogen and phosphorus loading reduced by more than 50 and 80%, respectively (Clarke et al., 2003; Staehr et al., 2017). Phytoplankton growth was likely to be nitrogen limited at the time of our samplings, especially in July (Riemann et al., 2016). Average chlorophyll a concentration was 4.5 μg l^{-1} between 2005 and 2014 (Staehr et al., 2017) and 2.8 μg l^{-1} during our study period, and dissolved organic carbon concentration was around 500 μmol l^{-1} in 2012-2016 (Asmala et al., 2019), but these values cannot fully account for the nutrient loading or eutrophication status of Roskilde Fjord. The high nutrient inputs in Roskilde Fjord do not result in high phytoplankton biomass (between 2 and 6 μg l^{-1} of chlorophyll a during our study period) due to complex ecosystem features, such as dense macrophyte beds -taking up nutrients- and mussel beds -taking up phytoplankton, explaining the above-mentioned high dissolved organic carbon concentration. Therefore, a large part of nutrients entering Roskilde Fjord are recycled rapidly within the system; these high nutrient inputs do not result in high phytoplankton biomass, with chlorophyll a peaking at less than 10 μg l^{-1} in early spring (Riemann et al., 2016; Staehr et al., 2017).

4.2. N_2O concentrations and fluxes in Roskilde Fjord

Water column N_2O concentrations had not been measured previously in the Roskilde Fjord, yet some values are available in other estuaries of the Scandinavian region. Table 3 summarizes the N_2O water concentrations in various estuaries.

For example in the Baltic Sea, values of a magnitude of 9.4 to 11.1 nmol kg^{-1} were reported at 3-22m depth (Wilson et al., 2018) and 11.8 to 24.4 nmol l^{-1} below 70 m (Myllykangas et al., 2017); 6-14 nmol N_2O l^{-1} were reported in the Southwestern Baltic Sea between 2006 and 2008 (Bange et al., 2009), and a similar value between 1991 and 1992 in the Central North Sea (Bange et al., 1996). Yet the N_2O concentrations in Roskilde Fjord were about 10 times lower than in the Seine estuary, strongly impacted by Paris conurbation, with at least 70 nmol N_2O l^{-1} (Garnier et al., 2006) or in the Elbe estuary (Brase et al., 2017).

The estimated N_2O fluxes at Roskilde Fjord (median of -0.04 nmol m^{-2} s^{-1}) fell within the lower end of previous observations of N_2O fluxes in estuaries in temperate regions: for instance, Livesley and Andrusiak (2012) reported, in a temperate estuary (Mornington Peninsula, Victoria Australia), a range of fluxes between -0.025 and 0.417 nmol m^{-2} s^{-1};

Table 3
N_2O water concentrations reported in the scientific literature.

Reference	Location, year, other details	Unit	Concentration	Type of values
Wilson et al. (2018)	Baltic Sea, 2016, 3 m depth	nmol N_2O kg^{-1}*	11.0-11.1	range of medians
	Baltic Sea, 2016, 21-22 m depth	nmol N_2O kg^{-1}*	9.4-9.6	range of medians
Myllykangas et al. (2017)	Baltic Sea, 2015, below 70m	nmol N_2O l^{-1}	11.8-24.4	volume-weighted average
Bange et al. (2009)	Baltic Sea, 2006-2008	nM N_2O**	6-14	
Bange et al. (1996)	Central North Sea, 1991	nmol l^{-1} N_2O	9.2	mean
	German Bight, 1991	nmol l^{-1} N_2O	8.66	mean
	German Bight, 1992	nmol l^{-1} N_2O	8.38	mean
	Gironde Estuary, 1991	nmol l^{-1} N_2O	14.3	area-weighted mean
Garnier et al. (2009, 2006)	Seine Estuary, 0-10 salinity, 1998-2003, France	nmol l^{-1} N_2O***	70-100	range
Garnier et al., unpublished	Seine Estuary, 20-33 salinity, 2001-2002, France	nmol l^{-1} N_2O***	14-53	range
Brase et al. (2017)	Elbe estuary, Hamburg port region, 2015, Germany	nM**	32.3-52.2	range
	Elbe estuary, 0 salinity, 2015, Germany	nM**	12-15	range
Bange et al. (2019)	Borneo estuaries, 2017	nmol N_2O l^{-1}*	2-41	range for six estuaries
Yevenes et al. (2017)	Reloncaví estuary, Chilean Patagonia, 2013, 0-5 m depth	nM**	11.8 ± 1.7	mean ± SD
Sánchez-Rodríguez et al. (2022)	Guadalquivir Estuary, 20-35 salinity, 2018 & 2019, Spain	nmol N_2O kg^{-1}*	10-20	range
This study	Roskilde Fjord, 2014, 1m depth	nmol N_2O l^{-1}	2.81-5.87	range of medians

* nmol N_2O kg^{-1} equivalent to nmol N_2O L^{-1} considering 1l = 1kg
** nM stands for nmol l^{-1}
*** μgN-N_2O l^{-1}, converted by the authors in nmol N_2O l^{-1}
SD stands for standard deviation

Garnier et al. (2009) reported a range of fluxes between 0.04 and 3.51 nmol m^{-2} s^{-1} in the Seine basin (France); and Foster and Fulweiler (2016) reported a mean (±sd) flux of -6 10^{-3} (±1 10^{3}) nmol m^{-2} s^{-1} in a shallow temperate estuary (Waquoit Bay, MA, USA).

Both the simplistic and quality-of-fit models had great predictive power. The estimated N_2O water concentrations differed substantially, but the N_2O fluxes derived from each model differed only marginally, probably because at every moment, all predicted N_2O concentrations were always lower than the equilibrium concentrations. It could be different in another estuary. Since our modeling approach was statistical and not deterministic, the models we present cannot be used 'as-is'

directly in other sites. Researchers willing to apply our methodology would have to find the coefficients that best fit their data.

4.3. Credibility of the N_2O fluxes in Roskilde Fjord

We believe our N_2O flux estimations at sampling point 2 (median fluxes of -0.05 and -0.04 nmol m^{-2} s^{-1} for the simplistic and the best-goodness-of-fit models, respectively) are credible for several reasons:

(1) The sampling point 2 – from which all N_2O water concentrations and N_2O fluxes were derived – was very similar to the 14 other sampling points over Roskilde Fjord in terms of salinity, temperature, DIP, etc. Therefore, estimates at this sampling point provide a likely magnitude of the fluxes occurring over the study area, as also supported by the sensitivity analyses.
(2) The tall tower measured fluxes coming from the whole landscape, in a 5-km radius including about 36 km^2 of the inner Roskilde Fjord and 24 km^2 of agricultural area, in addition to the city of Roskilde, with several other sources of N_2O such as an incinerator and a large wastewater treatment plant. When considering only the fluxes coming from the Western sector mainly occupied by Roskilde Fjord, we estimated a median landscape budget of 0.07 [-0.04, 0.21] nmol m^{-2} s^{-1}. This Western sector still includes parts of agricultural area intertwined in Roskilde Fjord, and we estimated an annual N_2O flux from the nearby agricultural area of 0.13-0.18 nmol m^{-2} s^{-1}. Therefore, the tall tower measurements fell in between the estimates from Roskilde Fjord and the nearby agricultural area. These estimates were derived from distinct methodologies and pertain to different scales: therefore, we cannot strictly compare them, yet they provide a promising basis to future research to validate our estimates and our methodology.

4.4. Possible mechanisms of N_2O synthesis

We had hypothesized that nitrogen variables would play a key role in the mechanisms involved in N_2O production, with a contribution of DIP as proxy for eutrophication. Yet our best quality-of-fit-model does not include any nitrogen variables as it yielded small and non-significant coefficients. This was unexpected, but several explanations are possible, such as the benthic remineralization of sedimentary organic P (Aller and Benninger, 1981; Sondergaard et al., 2013). Although benthic remineralization may not be directly linked to the N_2O production, it may act as a proxy for (i) oxic heterotrophic water column and sediment microbial respiration - *e.g.* ammonification followed by ammonium oxidation and possible associated N_2O emissions (Garnier et al., 2007; Ward et al., 2008), for (ii) oxygen depleted conditions in the sediments - *e.g.* the depth of the anoxic layer - which govern anaerobic respiration with NO_3 oxidation, *i.e.* denitrification and again N_2O production as an intermediate compound (Froelich et al., 1979). As previously reported, these conditions of eutrophication fit well with observed annual denitrification patterns (Piña-Ochoa and Álvarez-Cobelas, 2006). The role of DIP in this statistical modeling must be interpreted with caution: in addition to a possible mechanistic explanation as described above, DIP could be the proxy of an unmeasured variable related, for instance, to sediment anoxia. Despite nitrogen variables are closer to N_2O in the biological mechanisms, DIN concentrations in the water column do not always reflect the nitrogen transformation, as any 'free' DIN level is about two orders of magnitude higher than N_2O concentrations. However, we had no indicator of the sediment activity available (such as bottom oxygen level), over our 15 sampling sites to build our models. Since temperature controls most chemical reactions, including denitrification both in the water column and the sediments (Bouletreau et al., 2012; Klein et al., 2017), this may explain that temperature confounded nitrogen variables. Interestingly however, significant relationships between N_2O and NO_3 have been found in agricultural contaminated groundwaters (Vilain et al., 2012), where eutrophication *de facto* does not occur. However, using other proxy variables (specifically DIP), our models described well the variations of N_2O concentrations of our study and we are confident that the estimated concentrations are reasonable. Thus, contrary to a hypothesis of N_2O supersaturation due to efficient N-cycling in the Roskilde Fjord, the negative fluxes that we estimated may result from a very efficient denitrification to N_2 end-product, without N_2O intermediates in the anoxic sediment-water interface, which is made possible by the shallow water depths and sediment rich in bioavailable organic matter (Rönner, 1983).

4.5. Strengths, limitations, and general implications of the findings

Our study included 15 sampling points quite regularly distributed over the study area, allowing for a good overview of the spatial variability of the measured biotic and abiotic variables, at three different surveys accounting for different metabolic states of the Roskilde Fjord (spring, summer and autumn). Our modelling approach made it possible to account for the non-linear relationship between temperature and N_2O concentrations, providing time-series of N_2O concentrations from an interpolated long-term water monitoring station in the Roskilde Fjord. These calculated N_2O fluxes from the Roskilde Fjord also agree with the eddy covariance measurements on the tall tower nearby and the estimated N_2O fluxes from the agricultural landscape.

This study was limited by the lack of eddy covariance data in the first months of 2014, so we could not put in perspective the different estimated fluxes (Roskilde Fjord, eddy covariance, and agricultural area) over a complete year, and each method includes uncertainties in the estimation of N_2O.

Regarding the estimated N_2O fluxes in Roskilde Fjord, the complete approach relies on a series of assumptions. To start with, the predicted N_2O concentrations in water were derived from statistical modeling. The models showed each a high R^2 coefficient and the data feeding the models was consistent with the data from the long-term monitoring station 2, so that we chose dates that were representative of different key periods of Roskilde Fjord. Then, we used well-known equations to calculate equilibrium concentrations and to derive fluxes. The risk of error propagation cannot be excluded. For this reason, we compared these fluxes to measurements by other metrics calculated independently, such as those obtained at the tall tower.

Regarding measured fluxes at the tall tower, it remains difficult to clearly decipher between sources that may also have contributed to N_2O fluxes, for instance the incinerator of the Roskilde city. Since Roskilde Fjord is surrounded by agricultural areas or by the city, we cannot ascertain that the fluxes measured at the tall tower, which we attempted to constrain from the Northwest sector, were only coming from the Roskilde Fjord. In addition, we constrained the measurements to daytime to restrict the spatial coverage of the eddy covariance measurements to close to the 5-km radius footprint, but there was no way to ensure that fluxes did not come from further than 5 km from the tall tower. Therefore, a certain amount of noise might exist in this signal, due to the surrounding agricultural area.

Regarding N_2O fluxes from the nearby agricultural area, the calculations are based on major hypotheses: for the simplified IPCC calculations, we did as if all N-inputs were from synthetic fertilizers, while there was probably some manure. For this reason, we used another formula to obtain another independent estimation of average annual agricultural flux. In addition, using these annual agricultural fluxes in the comparison of N_2O fluxes in our study area has the following limitation: an annual average does not depict the seasonal variations of N_2O emissions that should be higher in early spring, depending on the dates of fertilizer applications (generally taking place at the beginning of the growing season).

Finally, we could not estimate N_2O fluxes in the Roskilde Fjord in spring, when nitrogen concentrations are higher but temperatures are lower. We cannot ascertain whether Roskilde Fjord was a sink or a source of N_2O before our study began.

As shown in Table 3, several estuaries known to be eutrophic are indeed a source of N_2O considering the atmospheric equilibrium concentration varying around 10 nmol l^{-1} (Weiss and Price (1980), taking into account the temperature). Given Roskilde Fjord remains a eutrophic estuary despite major improvements since the past decades, we had hypothesized it to be a source of N_2O. Yet, our findings suggest otherwise. Indeed, all estimated fluxes were negative, because, at each date and sampling point over the study period, N_2O water concentrations never exceeded equilibrium concentrations (Fig. 5). Therefore, our results suggest that Roskilde Fjord could be a sink of N_2O – at least during the study period. This would not be the first temperate estuary reported as a N_2O sink (Foster and Fulweiler, 2016). More research is thus needed to better quantify and understand N_2O budgets in estuaries, and to determine what makes some of them sinks for N_2O. The finding of undersaturation of N_2O raises important questions, most importantly on the extent to which other marine systems act as a sink for the greenhouse gas N_2O. Estuaries may contribute as high as 5% of the recent worldwide N_2O budget (Tian et al., 2020), but their emissions could be misestimated (Maavara et al., 2019). Therefore, we need more data and more tools to refine our current budget. Yet in terms of global budget, even though all estuaries would act as N_2O sinks (which does not seem realistic), this would decrease the estimated N_2O emissions by seemingly less than 5%. This also raises questions on the implications for the global budgets of other greenhouse gases (mostly CH_4, CO_2), but also on the mechanisms involved in N_2O sinks and sources. Indeed, N_2O undersaturation suggests that processes consuming N_2O are present in Roskilde Fjord. Bacterial consumption of N_2O has been observed in the Arctic, but it remains unknown how widespread this phenomenon is in marine systems (Rees et al., 2021). Finally, it raises the question of the conditions under which such mechanisms occur, and to which extent they would be present in other ecosystems. Better understanding this variety of mechanisms may help better quantify N_2O fluxes and adapt budgeting and designing local and global mitigation strategies.

5. Conclusions

- Between May and October 2014, Roskilde Fjord was a sink of N_2O, with a median flux of -0.04 nmol m^{-2} s^{-1} based on measured and modelled N_2O concentrations in the water, and on measured temperature, salinity, N_2O atmospheric concentration, and wind speed.
- Unexpectedly, including nitrogen variables in the modelling approach did not improve the model performance. Including dissolved inorganic phosphorus helped better capture the variation in N_2O concentrations, suggesting that P recycling (P adsorption-desorption, benthic redox conditions, uptake and mineralization, …) might be a better proxy than dissolved inorganic nitrogen specifically linked to (micro-) biological processes leading to N_2O production in specific conditions.
- In the period covered by both eddy covariance measurements and our modelling approach, we found compatible order of magnitude for the fluxes from Roskilde Fjord and from the agricultural landscape.
- Our modeling approach proves an efficient method to generate time-series of N_2O fluxes from a water body.
- The comparison between all estimates of N_2O fluxes should be interpreted with caution as it aimed only to internally corroborate the estimations from Roskilde Fjord, and includes some shortcomings (*e.g.*, the tall tower did not measure fluxes during the complete study period, and the calculated estimations for the agricultural area only provide a unique number, *i.e.* an annual average, serving only as order of magnitude).

Contributions

BL and RM provided the main financial and material support for the study and AI for the eddy covariance data (InGOS EU-FP7 project). JG and SM funded and supervised the surveys in the Roskilde Fjord and the chemical analyses. EL, EA, SM and JG designed the study. EL, EA, and SM carried out the three sampling campaigns. AI conducted the eddy covariance measurements and calculated fluxes. EL performed the statistical analyses and took the lead in drafting the manuscript and edited all subsequent drafts. EA, SM, JG, BL, RM and AI provided critical interpretations of the results. All authors contributed to interpreting the data, provided revisions to the manuscript, and approved the final draft.

Declaration of Competing Interest

The authors declare that they have no known competing financial interests or personal relationships that could have appeared to influence the work reported in this paper.

Data availability

Data will be made available on request.

Acknowledgments

This project was funded by European project FP7-Ingos. We are thankful to the colleagues who performed the chemical analyses in water samples and who help maintain the tall tower.

Supplementary materials

Supplementary material associated with this article can be found, in the online version, at doi:10.1016/j.watres.2022.118874.

References

Aller, R., Benninger, L., 1981. Spatial and temporal patterns of dissolved ammonium, manganese, and silica fluxes from bottom sediments of long-island-sound, USA. J. Mar. Res. 39, 295–314.

Asmala, E., Gustafsson, C., Krause-Jensen, D., Norkko, A., Reader, H., Staehr, P.A., Carstensen, J., 2019. Role of eelgrass in the coastal filter of contrasting Baltic Sea environments. Estuaries Coasts 42, 1882–1895. https://doi.org/10.1007/s12237-019-00615-0.

Asmala, E., Haraguchi, L., Markager, S., Massicotte, P., Riemann, B., Staehr, P.A., Carstensen, J., 2018. Eutrophication leads to accumulation of recalcitrant autochthonous organic matter in coastal environment. Glob. Biogeochem. Cycles 32, 1673–1687. https://doi.org/10.1029/2017GB005848.

Bange, H.W., 2006. Nitrous oxide and methane in European coastal waters. Estuar. Coast. Shelf Sci. 70, 361–374. https://doi.org/10.1016/j.ecss.2006.05.042.

Bange, H.W., Andreae, M.O., Lal, S., Law, C.S., Naqvi, S.W.A., Patra, P.K., Rixen, T., Upstill-Goddard, R.C., 2001. Nitrous oxide emissions from the Arabian Sea: a synthesis. Atmos. Chem. Phys. 1, 61–71. https://doi.org/10.5194/acp-1-61-2001.

Bange, H.W., Bell, T.G., Cornejo, M., Freing, A., Uher, G., Upstill-Goddard, R.C., Zhang, G., 2009. MEMENTO: a proposal to develop a database of marine nitrous oxide and methane measurements. Environ. Chem. 6, 195–197. https://doi.org/10.1071/EN09033.

Bange, H.W., Rapsomanikis, S., Andreae, M.O., 1996. Nitrous oxide in coastal waters. Glob. Biogeochem. Cycles 10, 197–207. https://doi.org/10.1029/95GB03834.

Bange, H.W., Sim, C.H., Bastian, D., Kallert, J., Kock, A., Mujahid, A., Müller, M., 2019. Nitrous oxide (N_2O) and methane (CH_4) in rivers and estuaries of northwestern Borneo. Biogeosciences 16, 4321–4335. https://doi.org/10.5194/bg-16-4321-2019.

Bie, M.J.M.de, Middelburg, J.J., Starink, M., Laanbroek, H.J., 2002. Factors controlling nitrous oxide at the microbial community and estuarine scale. Mar. Ecol. Prog. Ser. 240, 1–9. https://doi.org/10.3354/meps240001.

Borges, A.V., Darchambeau, F., Lambert, T., Bouillon, S., Morana, C., Brouyere, S., Hakoun, V., Jurado, A., Tseng, H.-C., Descy, J.-P., Roland, F.a.E., 2018. Effects of agricultural land use on fluvial carbon dioxide, methane and nitrous oxide concentrations in a large European river, the Meuse (Belgium). Sci. Total Environ. 610, 342–355. https://doi.org/10.1016/j.scitotenv.2017.08.047.

Bouletreau, S., Salvo, E., Lyautey, E., Mastrorillo, S., Garabetian, F., 2012. Temperature dependence of denitrification in phototrophic river biofilms. Sci. Total Environ. 416, 323–328. https://doi.org/10.1016/j.scitotenv.2011.11.066.

Brase, L., Bange, H.W., Lendt, R., Sanders, T., Dähnke, K., 2017. High resolution measurements of nitrous oxide (N_2O) in the Elbe estuary. Front. Mar. Sci. 4, 162. https://doi.org/10.3389/fmars.2017.00162.

Cauwet, G., 1999. Determination of dissolved organic carbon and nitrogen by high temperature combustion. In: Grasshoff, K., Kremling, K., Ehrhardt, nfred (Eds.), Methods of Seawater Analysis, Eds. Wiley-VCH Verlag GmbH, pp. 407–420. https://doi.org/10.1002/9783527613984.ch15.

Cébron, A., Garnier, J., Billen, G., 2005. Nitrous oxide production and nitrification kinetics by natural bacterial communities of the lowerSeine river (France). Aquat. Microb. Ecol. 41, 25–38. https://doi.org/10.3354/ame041025.

Chirinda, N., Carter, M.S., Albert, K.R., Ambus, P., Olesen, J.E., Porter, P.R., Petersen, S. O., 2010. Emissions of nitrous oxide from arable organic and conventional cropping systems on two soil types. Agric. Ecosyst. Environ. 136, 199–208. https://doi.org/10.1016/j.agee.2009.11.012.

Clarke, A., Juggins, S., Conley, D., 2003. A 150-year reconstruction of the history of coastal eutrophication in Roskilde Fjord, Denmark. Mar. Pollut. Bull. 46, 1615–1618. https://doi.org/10.1016/S0025-326X(03)00375-8.

Cloern, J.E., 2001. Our evolving conceptual model of the coastal eutrophication problem. Mar. Ecol. Prog. Ser. 210, 223–253. https://doi.org/10.3354/meps210223.

Conley, D.J., Markager, S., Andersen, J., Ellermann, T., Svendsen, L.M., 2002. Coastal eutrophication and the Danish national aquatic monitoring and assessment program. Estuaries 25, 848–861.

de Vries, W., Kros, J., Reinds, G.J., Butterbach-Bahl, K., 2011. Quantifying impacts of nitrogen use in European agriculture on global warming potential. Curr. Opin. Environ. Sustain. 3, 291–302. https://doi.org/10.1016/j.cosust.2011.08.009.

Eugster, W., Kling, G., Jonas, T., McFadden, J.P., Wuest, A., MacIntyre, S., Chapin, F.S., 2003. CO_2 exchange between air and water in an Arctic Alaskan and Midlatitude Swiss lake: importance of convective mixing. J. Geophys. Res. Atmos. 108, 4362. https://doi.org/10.1029/2002JD002653.

Flindt, M.R., Kamp-Nielsen, L., Marques, J.C., Pardal, M.A., Bocci, M., Bendoricchio, G., Salomonsen, J., Nielsen, S.N., Jørgensen, S.E., 1997. Description of the three shallow estuaries: Mondego River (Portugal), Roskilde Fjord (Denmark) and the Lagoon of Venice (Italy). Ecol. Model. Development of Models with Dynamic Structure for Marine Ecosystems 102, 17–31. https://doi.org/10.1016/S0304-3800(97)00092-6.

Foster, S.Q., Fulweiler, R.W., 2016. Sediment nitrous oxide fluxes are dominated by uptake in a temperate estuary. Front. Mar. Sci. 3 https://doi.org/10.3389/fmars.2016.00040.

Froelich, P., Klinkhammer, G., Bender, M., Luedtke, N., Heath, G., Cullen, D., Dauphin, P., Hammond, D., Hartman, B., Maynard, V., 1979. Early oxidation of organic-matter in pelagic sediments of the eastern equatorial Atlantic - suboxic diagenesis. Geochim. Cosmochim. Acta 43, 1075–1090. https://doi.org/10.1016/0016-7037(79)90095-4.

Garnier, J., Billen, G., Cebron, A., 2007. Modelling nitrogen transformations in the lower Seine river and estuary (France): impact of wastewater release on oxygenation and N_2O emission. Hydrobiologia 588, 291–302. https://doi.org/10.1007/s10750-007-0670-1.

Garnier, J., Billen, G., Vilain, G., Martinez, A., Silvestre, M., Mounier, E., Toche, F., 2009. Nitrous oxide (N_2O) in the Seine river and basin: observations and budgets. Agric. Ecosyst. Environ. 133, 223–233. https://doi.org/10.1016/j.agee.2009.04.024.

Garnier, J., Cebron, A., Tallec, G., Billen, G., Sebilo, M., Martinez, A., 2006. Nitrogen behaviour and nitrous oxide emission in the tidal Seine River estuary (France) as influenced by human activities in the upstream watershed. Biogeochemistry 77, 305–326. https://doi.org/10.1007/s10533-005-0544-4.

Garnier, J., Le Noë, J., Marescaux, A., Sanz-Cobena, A., Lassaletta, L., Silvestre, M., Thieu, V., Billen, G., 2019. Long-term changes in greenhouse gas emissions from French agriculture and livestock (1852–2014): From traditional agriculture to conventional intensive systems. Sci. Total Environ. 660, 1486–1501. https://doi.org/10.1016/j.scitotenv.2019.01.048.

Hergoualc'h, K., Akiyama, H., Bernoux, M., Chirinda, N., del Prado, A., Kasimir, A., MacDonald, J., Ogle, S., Regina, K., van der Weerden, T., 2019. N_2O emissions from managed soils, and CO_2 emissions from lime and urea application. 2019 Refinement to the 2006 IPCC Guidelines for National Greenhouse Gas Inventories.

Hinsby, K., Markager, S., Kronvang, B., Windolf, J., Sonnenborg, T.O., Thorling, L., 2012. Threshold values and management options for nutrients in a catchment of a temperate estuary with poor ecological status. Hydrol. Earth Syst. Sci. 16, 2663–2683. https://doi.org/10.5194/hess-16-2663-2012.

Holmes, R.M., Aminot, A., Kerouel, R., Hooker, B.A., Peterson, B.J., 1999. A simple and precise method for measuring ammonium in marine and freshwater ecosystems. Can. J. Fish. Aquat. Sci. 56, 1801–1808. https://doi.org/10.1139/cjfas-56-10-1801.

Ibrom, A., Dellwik, E., Larsen, S.E., Pilegaard, K., 2007. On the use of the Webb-Pearman-Leuning theory for closed-path eddy correlation measurements. Tellus Ser. B-Chem. Phys. Meteorol. 59, 937–946. https://doi.org/10.1111/j.1600-0889.2007.00311.x.

IPCC, 2013. Climate change 2013. In: Stocker, T.F., Qin, D., Plattner, G.-K, Tignor, M., Allen, S.K., Boschung, J., Nauels, A., Xia, Y., Bex, V., Midgley, P.M. (Eds.), The Physical Science Basis. Contribution of Working Group I to the Fifth Assessment Report of the Intergovernmental Panel on Climate Change, ed. Cambridge University PressCambridge, United Kingdom and New York, NY, USA.

IPCC, 2006. 2006 IPCC Guidelines for National Greenhouse Gas Inventories, Prepared by the National Greenhouse Gas Inventories Programme, IGES, Japan. ed. Buendia L., Miwa K., Ngara T. and Tanabe K., Eggleston H.S.

Klein, J.J.M.de, Overbeek, C.C., Jørgensen, C.J., Veraart, A.J., 2017. Effect of temperature on oxygen profiles and denitrification rates in freshwater sediments. Wetlands 37, 975–983. https://doi.org/10.1007/s13157-017-0933-1.

Knudsen-Leerbeck, H., Mantikci, M., Bentzon-Tilia, M., Traving, S.J., Riemann, L., Hansen, J.L.S., Markager, S., 2017. Seasonal dynamics and bioavailability of dissolved organic matter in two contrasting temperate estuaries. Biogeochemistry 134, 217–236. https://doi.org/10.1007/s10533-017-0357-2.

Kormann, R., Meixner, F.X., 2001. An analytical footprint model for non-neutral stratification. Bound. Layer Meteorol. 99, 207–224. https://doi.org/10.1023/A:1018991015119.

Livesley, S.J., Andrusiak, S.M., 2012. Temperate mangrove and salt marsh sediments are a small methane and nitrous oxide source but important carbon store. Estuar. Coast. Shelf Sci. 97, 19–27. https://doi.org/10.1016/j.ecss.2011.11.002.

Maavara, T., Lauerwald, R., Laruelle, G.G., Akbarzadeh, Z., Bouskill, N.J., Van Cappellen, P., Regnier, P., 2019. Nitrous oxide emissions from inland waters: Are IPCC estimates too high? Glob. Change Biol. 25, 473–488. https://doi.org/10.1111/gcb.14504.

Marescaux, A., Thieu, V., Garnier, J., 2018. Carbon dioxide, methane and nitrous oxide emissions from the human-impacted Seine watershed in France. Sci. Total Environ. 643, 247–259. https://doi.org/10.1016/j.scitotenv.2018.06.151.

Markager, S., Stedmon, C.A., Søndergaard, M., 2011. Seasonal dynamics and conservative mixing of dissolved organic matter in the temperate eutrophic estuary Horsens Fjord. Estuar. Coast. Shelf Sci. 92, 376–388. https://doi.org/10.1016/j.ecss.2011.01.014.

Morgenstern, K., 2000. Turbulent CO2-, H2O- and Energy Fluxes above a Mediterranean Oak and a Mountainous Spruce Forest Investigated by Eddy-Covariance Measurements.

Morin, T.H., Bohrer, G., Stefanik, K.C., Rey-Sanchez, A.C., Matheny, A.M., Mitsch, W.J., 2017. Combining eddy-covariance and chamber measurements to determine the methane budget from a small, heterogeneous urban floodplain wetland park. Agric. For. Meteorol. 237, 160–170. https://doi.org/10.1016/j.agrformet.2017.01.022.

Murray, R.H., Erler, D.V., Eyre, B.D., 2015. Nitrous oxide fluxes in estuarine environments: response to global change. Glob. Change Biol. 21, 3219–3245. https://doi.org/10.1111/gcb.12923.

Myhre, G., Shindell, D., Bréon, F.-M., Collins, W., Fuglestvedt, J., Huang, J., Koch, D., Lamarque, J.-F., Lee, D., Mendoza, B., Nakajima, T., Robock, A., Stephens, G., Takemura, T., Zhang, H., 2013. Anthropogenic and natural radiative forcing. In: Stocker, T.F., Qin, D., Plattner, G.-K., Tignor, M., Allen, S.K., Doschung, J., Nauels, A., Xia, Y., Bex, V., Midgley, P.M. (Eds.), Climate Change 2013: The Physical Science Basis. Contribution of Working Group I to the Fifth Assessment Report of the Intergovernmental Panel on Climate Change, Eds. Cambridge University Press, Cambridge, UK, pp. 659–740. https://doi.org/10.1017/CBO9781107415324.018.

Myllykangas, J.-P., Jilbert, T., Jakobs, G., Rehder, G., Werner, J., Hietanen, S., 2017. Effects of the 2014 major Baltic inflow on methane and nitrous oxide dynamics in the water column of the central Baltic Sea. Earth Syst. Dyn. 8, 817–826. https://doi.org/10.5194/esd-8-817-2017.

Pedersen, T.M., Sand-Jensen, K., Markager, S., Nielsen, S.L., 2014. Optical changes in a eutrophic estuary during reduced nutrient loadings. Estuaries Coasts 37, 880–892. https://doi.org/10.1007/s12237-013-9732-y.

Piña-Ochoa, E., Álvarez-Cobelas, M., 2006. Denitrification in aquatic environments: a cross-system analysis. Biogeochemistry 81, 111–130. https://doi.org/10.1007/s10533-006-9033-7.

Podgrajsek, E., Sahlee, E., Bastviken, D., Holst, J., Lindroth, A., Tranvik, L., Rutgersson, A., 2014. Comparison of floating chamber and eddy covariance measurements of lake greenhouse gas fluxes. Biogeosciences 11, 4225–4233. https://doi.org/10.5194/bg-11-4225-2014.

R Core Team, 2015. R: A language and environment for statistical computing. R Foundation for Statistical Computing, Vienna, Austria.

Rees, A.P., Brown, I.J., Jayakumar, A., Lessin, G., Somerfield, P.J., Ward, B.B., 2021. Biological nitrous oxide consumption in oxygenated waters of the high latitude Atlantic Ocean. Commun. Earth Environ. 2, 1–8. https://doi.org/10.1038/s43247-021-00104-y.

Riemann, B., Carstensen, J., Dahl, K., Fossing, H., Hansen, J.W., Jakobsen, H.H., Josefson, A.B., Krause-Jensen, D., Markager, S., Stæhr, P.A., Timmermann, K., Windolf, J., Andersen, J.H., 2016. Recovery of Danish coastal ecosystems after reductions in nutrient loading: a holistic ecosystem approach. Estuaries Coasts 39, 82–97. https://doi.org/10.1007/s12237-015-9980-0.

Rönner, U., 1983. Distribution, production and consumption of nitrous oxide in the Baltic Sea. Geochim. Cosmochim. Acta 47, 2179–2188. https://doi.org/10.1016/0016-7037(83)90041-8.

Sánchez-Rodríguez, J., Sierra, A., Jiménez-López, D., Ortega, T., Gómez-Parra, A., Forja, J., 2022. Dynamic of CO_2, CH_4 and N_2O in the Guadalquivir estuary. Sci. Total Environ. 805, 150193 https://doi.org/10.1016/j.scitotenv.2021.150193.

Schubert, C.J., Diem, T., Eugster, W., 2012. Methane emissions from a small wind shielded lake determined by eddy covariance, flux chambers, anchored funnels, and boundary model calculations: a comparison. Environ. Sci. Technol. 46, 4515–4522. https://doi.org/10.1021/es203465x.

Smith, K.A., 2017. Changing views of nitrous oxide emissions from agricultural soil: key controlling processes and assessment at different spatial scales. Eur. J. Soil Sci. 68, 137–155. https://doi.org/10.1111/ejss.12409.

Sondergaard, M., Bjerring, R., Jeppesen, E., 2013. Persistent internal phosphorus loading during summer in shallow eutrophic lakes. Hydrobiologia 710, 95–107. https://doi.org/10.1007/s10750-012-1091-3.

Staehr, P.A., Testa, J., Carstensen, J., 2017. Decadal changes in water quality and net productivity of a shallow Danish estuary following significant nutrient reductions. Estuaries Coasts 40, 63–79. https://doi.org/10.1007/s12237-016-0117-x.

Tallec, G., Garnier, J., Billen, G., Gousailles, M., 2006. Nitrous oxide emissions from secondary activated sludge in nitrifying conditions of urban wastewater treatment plants: effect of oxygenation level. Water Res. 40, 2972–2980. https://doi.org/10.1016/j.watres.2006.05.037.

Tian, H., Xu, R., Canadell, J.G., Thompson, R.L., Winiwarter, W., Suntharalingam, P., Davidson, E.A., Ciais, P., Jackson, R.B., Janssens-Maenhout, G., Prather, M.J., Regnier, P., Pan, N., Pan, S., Peters, G.P., Shi, H., Tubiello, F.N., Zaehle, S., Zhou, F., Arneth, A., Battaglia, G., Berthet, S., Bopp, L., Bouwman, A.F., Buitenhuis, E.T., Chang, J., Chipperfield, M.P., Dangal, S.R.S., Dlugokencky, E., Elkins, J.W., Eyre, B. D., Fu, B., Hall, B., Ito, A., Joos, F., Krummel, P.B., Landolfi, A., Laruelle, G.G., Lauerwald, R., Li, W., Lienert, S., Maavara, T., MacLeod, M., Millet, D.B., Olin, S., Patra, P.K., Prinn, R.G., Raymond, P.A., Ruiz, D.J., van der Werf, G.R., Vuichard, N., Wang, J., Weiss, R.F., Wells, K.C., Wilson, C., Yang, J., Yao, Y., 2020.

A comprehensive quantification of global nitrous oxide sources and sinks. Nature 586, 248–256. https://doi.org/10.1038/s41586-020-2780-0.

Turner, P.A., Griffis, T.J., Lee, X., Baker, J.M., Venterea, R.T., Wood, J.D., 2015. Indirect nitrous oxide emissions from streams within the US Corn Belt scale with stream order. Proc. Natl. Acad. Sci. 112, 9839–9843. https://doi.org/10.1073/pnas.1503598112.

Vilain, G., Garnier, J., Tallec, G., Tournebize, J., 2012. Indirect N2O emissions from shallow groundwater in an agricultural catchment (Seine Basin, France). Biogeochemistry 111, 253–271. https://doi.org/10.1007/s10533-011-9642-7.

Ward, B.B., Tuit, C.B., Jayakumar, A., Rich, J.J., Moffett, J., Naqvi, S.W.A., 2008. Organic carbon, and not copper, controls denitrification in oxygen minimum zones of the ocean. Deep Sea Res. Part Oceanogr. Res. Pap. 55, 1672–1683. https://doi.org/10.1016/j.dsr.2008.07.005.

Weiss, R., Price, B., 1980. Nitrous-oxide solubility in water and seawater. Mar. Chem. 8, 347–359. https://doi.org/10.1016/0304-4203(80)90024-9.

Wilson, S.T., Bange, H.W., Arévalo-Martínez, D.L., Barnes, J., Borges, A.V., Brown, I., Bullister, J.L., Burgos, M., Capelle, D.W., Casso, M., Paz, M.de la, Farías, L., Fenwick, L., Ferrón, S., Garcia, G., Glockzin, M., Karl, D.M., Kock, A., Laperriere, S., Law, C.S., Manning, C.C., Marriner, A., Myllykangas, J.-P., Pohlman, J.W., Rees, A. P., Santoro, A.E., Tortell, P.D., Upstill-Goddard, R.C., Wisegarver, D.P., Zhang, G.-L., Rehder, G., 2018. An intercomparison of oceanic methane and nitrous oxide measurements. Biogeosciences 15, 5891–5907. https://doi.org/10.5194/bg-15-5891-2018.

Wood, S., 2006. Generalized Additive Models: An Introduction with R, ed. Chapman and Hall/CRC.

Yevenes, M.A., Bello, E., Sanhueza-Guevara, S., Farías, L., 2017. Spatial distribution of nitrous oxide (N_2O) in the Reloncaví estuary–sound and adjacent sea (41°–43° S), Chilean patagonia. Estuaries Coasts 40, 807–821. https://doi.org/10.1007/s12237-016-0184-z.

Zuur, A.F., Ieno, E.N., Walker, N.J., Saveliev, A.A., Smith, G.M., 2009a. Mixed Effects Modelling for Nested Data. In: Zuur, A.F., Ieno, E.N., Walker, N., Saveliev, A.A., Smith, G.M. (Eds.), Mixed Effects Models and Extensions in Ecology with R, Statistics for Biology and Health, Eds. Springer, New York, NY, pp. 101–142. https://doi.org/10.1007/978-0-387-87458-6_5.

Zuur, A.F., Ieno, E.N., Walker, N.J., Saveliev, A.A., Smith, G.M., 2009b. GLMM and GAMM. In: Zuur, A.F., Ieno, E.N., Walker, N., Saveliev, A.A., Smith, G.M. (Eds.), Mixed Effects Models and Extensions in Ecology with R, Statistics for Biology and Health, Eds. Springer, New York, NY, pp. 323–341. https://doi.org/10.1007/978-0-387-87458-6_13.